Fabrication of $LaFeO_3$ and rGO-$LaFeO_3$ Microspheres based Gas Sensors for Detection of NO_2 and CO

Neeru Sharma[1*], Himmat Singh Kushwaha[2], S.K.Sharma[1], K.Sachdev[1,2,*]

[1]Department of Physics, Malaviya National Institute of Technology, Jaipur 302017 (India)

[2]Materials Research Centre, Malaviya National Institute of Technology, Jaipur 302017 (India)

*Corresponding author Email: neerupathak93@gmail.com, ksachdev.phy@mnit.ac.in

In current report $LaFeO_3$ and rGO-$LaFeO_3$ were synthesized by hydrothermal method and device were fabricated by photolithography technique for detection of different concentration of CO and NO_2 gases at 200 and 250 ºC temperatures. Both synthesized microsphere shaped samples were characterized by XRD, Raman, FTIR, TGA, AFM, FESEM, XPS, TEM, UV-Vis, BET, among them some supporting information are presented here.

Raman Studies:

Figure S1 (a) and (b) shows the Raman spectra for $LaFeO_3$ and rGO-$LaFeO_3$ at room temperature, to get the information about order-disorder effect in lattice. The bands at around 141, 220, 287, 389, 491, 603, 1303 cm^{-1} are corresponding to $LaFeO_3$. The bands were observed at 141, 220, 287, 389, 491, 603 and 1303 cm^{-1} for $LaFeO_3$ shown in fig. S1 (a). The two major modes at 287 and 603 cm^{-1} attributed to Ag assign mode, two-photon and impurity scattering[1]. The band at 389 cm^{-1} assigned to B_{3g} mode while 491cm^{-1} assign to one-phonon scattering[2]. The band centered at 1303 corresponding to two-phonon scattering. The bands at 141and 220 may be due to some Fe_2O_3 impurity. Similar behavior was observed for rGO-$LaFeO_3$ shown in Fig. S1 (b), but higher shifting in wavenumber like 662 cm^{-1} is may be due to the reduction of GO. An additional peak appeared at 1699 cm^{-1} which is induced defect mode (D') scatter from K to K (K-point of Brillouin zone) [3,4], it may be splitting of G band by interaction of vibration mode of impurity with phonon mode of rGO.

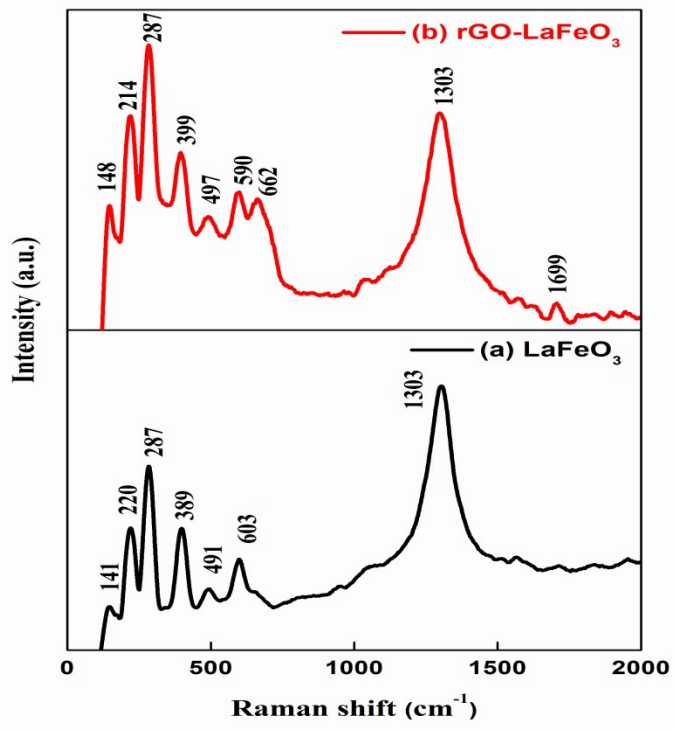

Fig. S1 Raman spectra for $LaFeO_3$ (a) and rGO-$LaFeO_3$ (b)

Thermal Studies:

TGA curve of $LaFeO_3$ and rGO-$LaFeO_3$ shown in Fig. S2 observed three weight loss segments. It can be seen that first weight loss about 100ºC was due to elimination of water molecule and crystallization of material. The second loss was observed between 220-389ºC due to decomposition of organic compound C-H and C=O. The third weight loss was above 520ºC may be due to decomposition of nitrate ions. After 730ºC no weight loss was observed which confirm possibility of formation of metal oxide phase of $LaFeO_3$

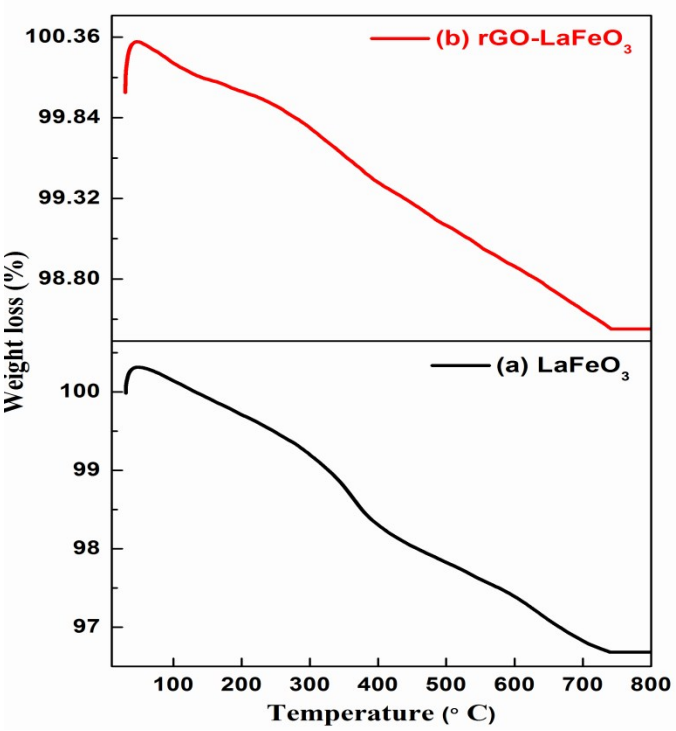

Fig. S2 TGA for $LaFeO_3$ (a) and rGO-$LaFeO_3$ (b)

Elemental Study:

Figure S3 (a) and (b) shows the EDAX spectra for $LaFeO_3$ and its composite with rGO (rGO-$LaFeO_3$) confirm the presence of element in respective samples. EDAX spectra of $LaFeO_3$ confirm the presence of La, Fe, and Oxygen in the multilayer structure in table S1 while EDAX spectra for rGO-$LaFeO_3$ shown in fig. S3 (b) confirmed that La, Fe, O, and carbon were present in that composite describe in table S2. EDAX spectra for rGO-$LaFeO_3$ shows higher signal of C which indicate large content of rGO.

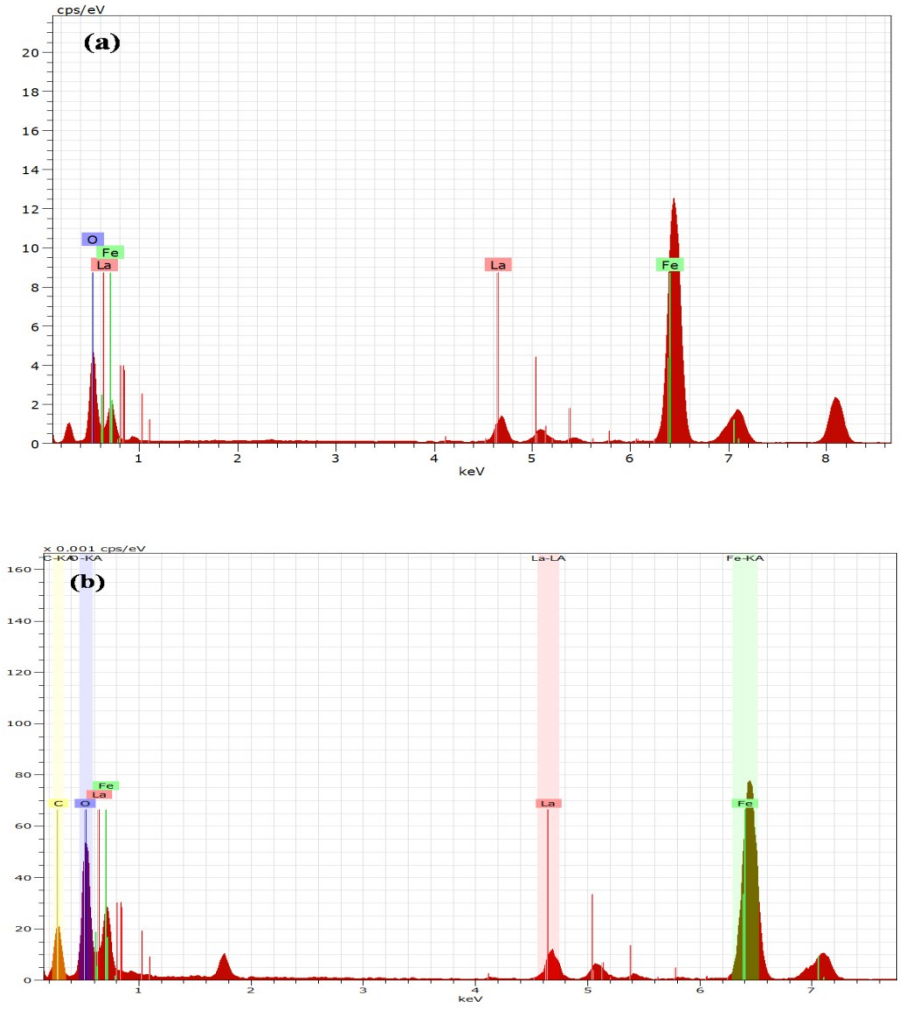

Fig. S3 EDAX spectra of $LaFeO_3$ (a) and rGO-$LaFeO_3$ (b)

Table S1.	**Elemental composition of $LaFeO_3$ by EDAX spectra**				
Elements	Series	Unn. [wt. %]	C norm. [wt.%]	C Atom [at. %]	C Error [wt. %]
Fe	K-series	65.72	65.72	49.87	2.01
La	L-series	17.34	17.34	5.29	1.77
O	K-series	16.93	16.93	44.84	0.55

Table S2.	**Elemental composition of rGO-$LaFeO_3$ by EDAX spectra**				
Elements	Series	Unn. [wt. %]	C norm. [wt.%]	C Atom [at. %]	C Error [wt. %]
Fe	K-series	34.14	34.14	12.67	1.09
La	L-series	12.31	12.31	1.84	1.29
O	K-series	16.03	16.03	20.76	0.55
C	K-series	37.52	37.52	64.74	1.45

Atomic Force Microscopy Studies:

The surface analysis of $LaFeO_3$ and rGO-$LaFeO_3$ using AFM with scan area 1× 1 μm^2 shown in fig. S4 (a) and (b) respectively. The root mean square (RMS) roughness of $LaFeO_3$ and rGO-$LaFeO_3$ were 0.707 nm and 6.73 nm respectively. This increment in roughness indicates growth of $LaFeO_3$ on GO sheets. Higher surface roughness of rGO-$LaFeO_3$ can enhance the sensing properties as it is directly proportional gas sensitivity. Larger roughness results in larger contact area with the gaseous species, this demonstrates the importance of surface to volume ratio in gas sensing application[5,6].

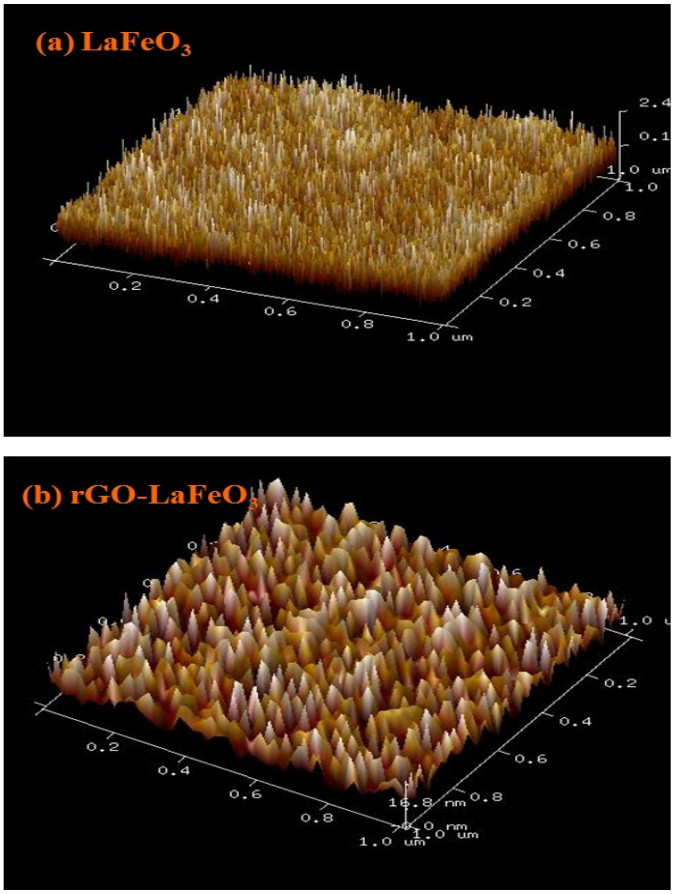

Fig. S4 AFM images-3D view of $LaFeO_3$ (a) and rGO-$LaFeO_3$ (b)

Gas Sensing Mechanism;

Carbon Mono Oxide (CO)

Gas sensing mechanism of $LaFeO_3$ for CO detection can be introduced by the following equation [7], this will be same for rGO-$LaFeO_3$;

(1) Oxygen molecules in atmosphere adsorb on the $LaFeO_3$ surface and form O^-(ads) by attracting electron from the conduction band of $LaFeO_3$ and gives following reaction.

$$O_2\,(gas) \rightarrow O_2\,(ads) \qquad (1)$$

$$O_2\,(ads) + 2e^- \rightarrow 2O^-\,(ads) \qquad (2)$$

This increase number of holes in the valance band, which decrease the resistance of p- type $LaFeO_3$.

(2) When CO (reducing gas) exposed to $LaFeO_3$, a reaction take place between CO and O^- such way;

$$CO\ (g) \rightarrow CO\ (ads) \quad (3)$$

$$CO\ (ads) + O^- \rightarrow CO_2 + e^- \quad (4)$$

Electrons are injected into the valance band and combine with hole which leads to decrease holes concentration and produce increase in the resistance.

Nitrogen dioxide (NO_2)

The gas sensing mechanism of $LaFeO_3$ with CO and NO_2 takes place as per following ways;

(1) NO_2 molecules capture electrons from $LaFeO_3$ surface, and form NO_2^- (ads). Which shows accepting behavior of NO_2[6].

$$NO_2\ (gas) + e^- \rightarrow NO_2^-\ (ads) \quad (5)$$

(2) NO_2 molecule having unpaired electron react with dangling bond on $LaFeO_3$ surface and capture a lone-pair electron from that which results formation of hole. This increment of hole concentration leads to decrease $LaFeO_3$ resistance and resistance recover to its initial value [6].

$$LaFeO_3^+ — NO_2^-\ (ads) \rightarrow LaFeO_3 — NO_2(ads) + h \quad (6)$$

Gas sensing comparison table:

Table S3. CO and NO_2 sensitivity of $LaFeO_3$ and rGO-$LaFeO_3$ comparison with already published research papers

Sample	Test gas	Concentration (ppm)	Temperature (ºC)	S (%)	Reference(Year)
$LaFeO_3$	CO	500	270	0.65	2003[8]
$LaFeO_3$	CO	500	RT	5	2011[9]
$LaFeO_3$	**CO**	**5**	**250**	**30.9**	**Current study**
rGO-$LaFeO_3$	**CO**	**5**	**250**	**31.9**	**Current study**
$LaFeO_3$ nanocube	NO_2	1	25	10.40	2014[6]
$LaFeO_3$	NO_2	5	150	80.4	2018[10]

$LaFeO_3$	**NO_2**	**3**	**250**	**144.1**	**Current study**
rGO-$LaFeO_3$	**NO_2**	**3**	**250**	**183.4**	**Current study**

1 S. Thirumalairajan, K. Girija, V. Ganesh, D. Mangalaraj, C. Viswanathan and N. Ponpandian, *Cryst. Growth Des.*, 2013, **13**, 291–302.

2 S. Thirumalairajan, K. Girija, I. Ganesh, D. Mangalaraj, C. Viswanathan, A. Balamurugan and N. Ponpandian, *Chem. Eng. J.*, 2012, **209**, 420–428.

3 J.-B. Wu, M.-L. Lin, X. Cong, H.-N. Liu and P.-H. Tan, *Chem. Soc. Rev.*, , DOI:10.1039/C6CS00915H.

4 I. Childres, L. Jauregui, W. Park, H. Cao and Y. Chen, *New Dev. Phot. Mater. Res.*, 2013, 1–20.

5 J. Zhao, Y. Liu, X. Li, G. Lu, L. You, X. Liang, F. Liu, T. Zhang and Y. Du, *Sensors Actuators, B Chem.*, 2013, **181**, 802–809.

6 S. Thirumalairajan, K. Girija, V. R. Mastelaro and N. Ponpandian, *Appl. Mater. $ Interfaces*, 2014, **6**, 13917–13927.

7 P. Song, Q. Wang, Z. Zhang and Z. Yang, *Sensors Actuators B. Chem.*, 2010, **147**, 248–254.

8 N. N. Toan, S. Saukko and V. Lantto, *Phys. B Condens. Matter*, 2003, **327**, 279–282.

9 P. Song and Q. Wang, *Mater. Sci. Forum*, 2011, **677**, 375–378.

10 M. L. P. H. Micro-, X. Zhang, W. Zhang and Z. Cai, *Ceram. Int.*, , DOI:10.1016/j.ceramint.2018.11.221.